Divided shifted Raman spectroscopy for carotenoid detection

S. D. Bergeson[a], J. B. Peatross[b], N. J. Eyring[b], J. F. Fralick[b], S. B. Ferguson[b]

[a] Department of Physics and Astronomy, Brigham Young University, Provo, UT 84602;
[b] Pharmanex Research Institute, 75 West Center, Provo, UT 84601 USA

ABSTRACT

We have developed a compact portable instrument for resonance Raman spectroscopy of carotenoid molecules in skin tissue. Our application focuses on the 1525 cm^{-1} Raman line common to all carotenoids. We use a divided shifted Raman spectroscopy (DSRS) technique that reduces sensitivity to detector drift and error. Two wavelength-narrowed LEDs illuminate the sample, and scattered light in four different wavelength channels is measured. This multi-spectral approach has single-photon sensitivity and compares favorably with laser-based Raman measurements in terms of accuracy, repeatability, and measurement time.

Keywords: resonance Raman spectroscopy, carotenoids, β-carotene, light emitting diodes

1. INTRODUCTION

A few years ago we developed a compact portable instrument for resonance Raman measurements of carotenoids in skin tissue. That instrument used a 473 nm frequency doubled Nd:YAG laser as the excitation source and a CCD-based spectrometer as a detector. Optical fibers were used to send light to the skin tissue and to collect fluorescence, similar to many Raman spectrometers in the literature.[1–7] While successful in a commercial setting, the instrument required extremely stable ambient operating conditions and used a somewhat cumbersome calibration procedure.

More recently we launched a project to build a Raman spectrometer using light emitting diodes as the excitation source. These sources can be much more compact and rugged than diode-pumped solid state lasers, and much less expensive than commercially available blue laser diodes. Compared to lasers, these sources have low spectral brightness. They emit over extended spatial regions, making it difficult to couple them directly into fiber optics, and they have limited optical output power. However, with proper optical design, detector choice, and analysis algorithms, these shortcomings can be overcome.

In this paper we describe the technical details of the optical design and data analysis of our instrument. We use two bandpass filtered LEDs to excite the Raman line, and measure the fluorescence in four simultaneous analysis channels. With this configuration we implement a method that we call divided shifted Raman spectroscopy (DSRS) in order to observe a weak Raman line on top of a large fluorescence background. The new LED Raman spectrometer compares favorably to more traditional laser instruments, and it can maintain its calibration for time periods approaching one year and perhaps longer.

2. CAROTENOID SPECTROSCOPY

The optical properties of carotenoids have been studied extensively using a variety of fluorescence, excited state absorption, and Raman methods.[8] Lycopene and β-carotene are the dominant carotenoids in skin tissue, and have similar optical response.[3] They have a backbone of nine conjugated carbon bonds, with additional conjugation into the ionone rings on each end. They both have strong absorption bands in the blue-green spectral region between 400 and 500 nm.

In β-carotene, the three dominant Raman lines are at 1008 cm^{-1} (C$-CH_3$ rocking mode), 1159 cm^{-1} (C$-$C stretch mode), and 1525 cm^{-1} (C=C stretch mode), with the latter being the strongest. Because of fast non-radiative relaxation, spontaneous fluorescence is suppressed, with a fluorescence quantum yield of only 10^{-5}.[2,9] However, in typical skin measurements the Raman signal is a small fraction of the total signal ($\sim$1%). Most of the fluorescence comes from other tissue components (lipids, proteins, melanin,

Biomedical Optical Spectroscopy, edited by Anita Mahadevan-Jansen, Wolfgang Petrich, Robert R. Alfano, Alvin Katz, Proc. of SPIE Vol. 6853, 68530A, (2008) · 1605-7422/08/$18 · doi: 10.1117/12.765195

Downloaded From: http://proceedings.spiedigitallibrary.org/ on 03/18/2014 Terms of Use: http://spiedl.org/terms

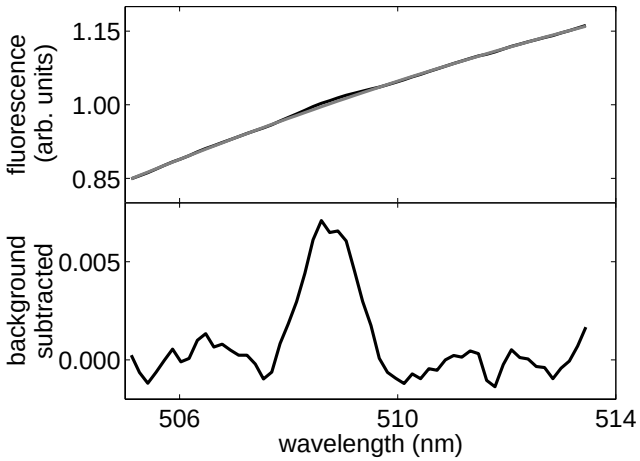


Figure 1. Top panel: Fluorescence signal from a hand under 473 nm laser excitation (black line) and a fit to the background (gray line) Bottom panel: the background subtracted Raman line.

DNA, hemoglobin, etc.[10]). Ideally, an instrument should have a signal-to-noise ratio of 10^4. At the same time, it must have high sensitivity since the detection rate is roughly 1 Raman photon per billion excitation photons, assuming $f/1$ collection optics.

3. LASER VS. LED EXCITATION

A typical spectrum of hand fluorescence is shown in Fig. 1 using 473 nm laser excitation. The signal-to-background ratio is around 0.005 (top panel). With appropriate background subtraction, the peak near 509 nm is more readily apparent (bottom panel).

The spectrum in Fig. 1 is instrument broadened. The excitation spectrum is a delta-function, but the spectrometer has roughly 1 nm resolution. When the excitation spectrum is broader, the signal-to-background level becomes even smaller. An 0.8 nm bandwidth excitation spectrum gives a 1 nm wide Raman line, and the signal to background level drops by another factor of 2.

When using an LED excitation source, the spectral measurements are much more difficult. The laser in Fig. 1 was 5 mW focused to about 0.5 mm diameter. Our filtered LED source is 0.5 mW focused to 2 mm diameter. The intensity is reduced by a factor of 80, giving an impractically low light level coupled into the spectrometer. Obviously a new spectral detector design is needed.

This lower signal level can be overcome in part by using a more sensitive detectors, such as a PMT. A filter-based instrument using PMT detection was reported.[11] Tilting the filter shifts (and broadens) the passband, and provided enough spectral discrimination to estimate the background level. In skin tissue, in which the signal-to-background ratio is roughly 50x smaller than in the macula, a more stable method must be used.

4. DUAL WAVELENGTH EXCITATION

The design of our LED instrument was based on measurements we made using two laboratory lasers. Figure 2 shows hand fluorescence and the 1525 cm^{-1} Raman line in a hand excited by a frequency doubled Nd:YAG laser at 473 nm and by an argon-ion laser at 476 nm.

The standard shifted subtracted Raman spectroscopy (SSRS) method would analyze this data by taking the difference of these spectra.[12] As shown in the middle panel of Fig. 2, this gives a characteristic lineshape that is free of spectral artifacts due to the spectrometer. The background is dominated by

Downloaded From: http://proceedings.spiedigitallibrary.org/ on 03/18/2014 Terms of Use: http://spiedl.org/terms

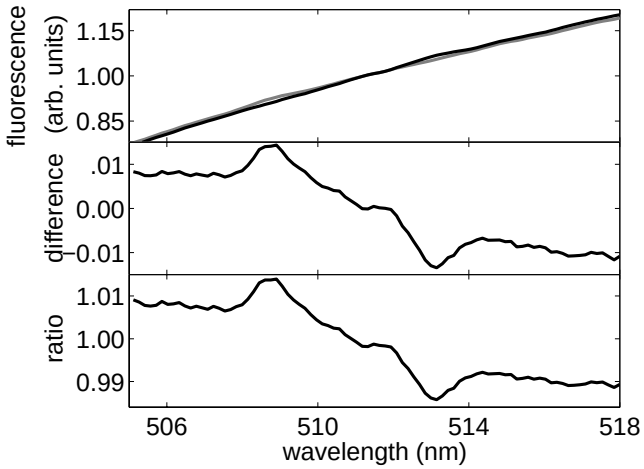


Figure 2. Hand fluorescence using two different excitation lasers. One laser is a frequency doubled Nd:YAG laser at 473 nm. The other is an argon ion laser at 476 nm. Top panel: hand fluorescence. Middle panel: difference spectrum (SSRS analysis). Bottom panel: ratio of spectra (DSRS analysis). Note that DSRS and SSRS signals have essentially identical signal to noise ratios and signal visibilities. The SSRS signal is centered at zero intensity. The DSRS spectrum is centered around 1.0

changes in detector sensitivity, amplifier gain, and dark signal, as well as real changes in the fluorescence spectra of the two excitation sources.

The ratio of the two Raman spectra gives the DSRS spectrum. The lineshape is very similar to the SSRS signal. Instead of being centered around zero, the spectrum is now centered around 1. But the overall signal to noise ratio and signal visibility is the same. If the two spectra can be measured on a short time scale, the variations in detector sensitivity and amplifier gain can be divided out. In some linear array detectors, where there is a significant even/odd amplifier effect, this can be important. One of the Raman spectra can serve as the flat field of the other spectrum.

5. OPTICAL LAYOUT

The optical layout has been described elsewhere.[13] It is optimized for detecting the 1525 cm^{-1} Raman line in skin tissue using resonance excitation. Using LEDs with interference filters gives us the flexibility to choose the excitation wavelength more or less arbitrarily. The optical layout is shown in Fig. 3. Light from a blue LED passes through an 0.8 nm bandwidth bandpass filter at 473 nm. This light reflects from a dichroic mirror and is focused onto the sample. Fluorescence and the Raman signal from the sample passes back through the dichroic mirror. A series of polarization-independent partially reflecting beam splitters divides the optical signal into four channels. Light in each channel passes through a 1 nm bandpass filter and is detected using a photomultiplier tube (PMT). The filters in front of the PMTs have centers spaced equally on 2 nm intervals. The center wavelengths of the detection filters are chosen so that one of the filters is shifted 1525 cm^{-1} from the excitation source, with one filter 2 nm to the red and two filters to the blue. For excitation at 473.0 nm, the detection filters are at 505.8 nm, 507.8 nm, 509.8 nm, and 511.8 nm. The 509.8 nm filter is centered on the Raman line. The other filters characterize the background fluorescence level.

We build a second Raman spectrometer into the same optical system. The second excitation source at 471.3 nm generates a Raman line at the 507.8 nm filter. As before, we have one detection filter centered on the Raman line straddled by three "background" filters to help establish the baseline.

The PMT gain is sensitive to changes in the operating voltage, the ambient temperature, and the spatial distribution of light on the photocathode. We have measured 20% changes in the detection efficiency over

Downloaded From: http://proceedings.spiedigitallibrary.org/ on 03/18/2014 Terms of Use: http://spiedl.org/terms

a few hours due to heating of the dynodes as the resistor chain warms up. This translates into a change of the signal level of 0.2×10^{-4} per second of measurement time. This complicates measurements that need to be accurate at the 10^{-4}, and makes it impossible to use standard flat fielding techniques (i.e.: dividing the measurement from a spectrally smooth sample into subsequent measurements).

The solution is to use the ratio of the two spectra. We measure the two spectra at a frequency of 5 Hz and average this ratio for 90 seconds. All rapid changes in the detector efficiency, as well as geometrical factors in the optical system) divide out. This would not be true in the difference. In this particular application, dividing is much more successful than subtracting.

When using two independent excitation sources, it is important to make sure that the spatial profile of the two sources is identical. Variations in this profile result from both the structure of the LEDs themselves but also in the interference filters used to narrow their output spectrum. We homogenize the excitation beams using a 1 mm diameter, 20 mm long glass rod. The material was chosen to have a high index of refraction and a low fluorescence level. This rod acts somewhat like a very large diameter optical fiber. The multiple internal reflections remove residual differences in the spatial profile of the two excitation sources. It is also important to make sure the optical polarization of the two sources is identical, and to make sure that the polarization is identical at each PMT. The Raman signal has the same polarization as the excitation source. This is not true for the background fluorescence. If the collected fluorescence at each PMT is not identical, a different signal to background ratio will be measured and the derived Raman signal strength will be compromised. Special care must be taken in choosing beam splitters because the Fresnel reflection coefficients at 45 degrees angle of incidence are typically quite different for the two polarizations in commercial beam splitters. This instrument needs to reliably measure fluorescence at the 10^{-4} level. Therefore controlling the spatial profile and polarization is critical to successful implementation of this approach.

The division technique described in this paper requires a simple Raman spectrum. The background measurement points need to be free of any Raman lines. It is ideal for situations in which the light levels are low and the fluorescence levels are high.

6. DSRS DATA ANALYSIS

The basic data analysis has been reported elsewhere.[13] For illustrative purposes, two simulated Raman signals are shown in the top panel of Fig. 4. The spectral windows measured by each of the four detection

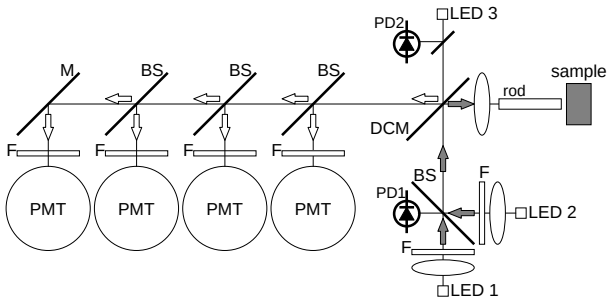


Figure 3. Schematic of the optical layout of our instrument. M = mirror, BS = beam splitter, DCM = dichroic mirror, F = bandpass filter, L = lens, PD = photodiode. Bandpass filter properties are noted in the text. The optical power at the sample is less than 0.5 mW in 3.1 mm^2.

Downloaded From: http://proceedings.spiedigitallibrary.org/ on 03/18/2014 Terms of Use: http://spiedl.org/terms

channels are also shown. The dashed line is the Raman signal using 473.0 nm excitation. The Raman peak appears in the third detector and the other three detectors record background levels. The gray line shows the Raman signal using 471.3 nm excitation. In this case the Raman peak appears in the second detector and the other three detectors record background levels. The black line shows the ratio of the two spectra. The lower panel of Fig. 4 shows the ratio of the optical signal measured by each detector.

We establish the baseline in the DSRS spectrum using the endpoints, which are always "background" measurements. We further constrain the baseline by assuming that the ratio measurement in detector 2 is as far above the baseline as the ratio measurement in detector 3 is below it. These assumptions yield a coupled system of equations for the background and signal strength:

$$\begin{aligned} y_1 &= a + bx_1 + cx_1^2 \\ y_2 &= a + bx_2 + cx_2^2 + d \\ y_3 &= a + bx_3 + cx_3^2 - d \\ y_4 &= a + bx_4 + cx_4^2 \end{aligned} \tag{1}$$

where y_i are the ratios of PMT measurements of the two excitation sources, and the x_i are the interference filter passband centers. The parameters a, b, and c are the coefficients of the parabola that best represents the baseline. The parameter d is magnitude of the difference between the Raman signal and the baseline on this relative scale. Note that these equations are derived assuming that d is small (e.g., d less than about 0.01 as for skin measurements).

When d approaches unity, higher-order terms in the calculation must be included. In line 2 of Eq. 1 we explicitly assumed that $y/(1 + d/y) = y - d$. However, when d becomes large more terms in the binomial expansion must be used. Of course, a large d means that the signal is large enough compared to the background that it can probably be reliably measured using more standard Raman spectroscopy methods.

The parameter d is put on an absolute scale by multiplying it by the PMT voltages used in the denominator of y_i. To achieve a good reliability, the detector stability needs only to be maintained (or measured) at the few percent level, which is much simpler than the 10^{-4} required without using the

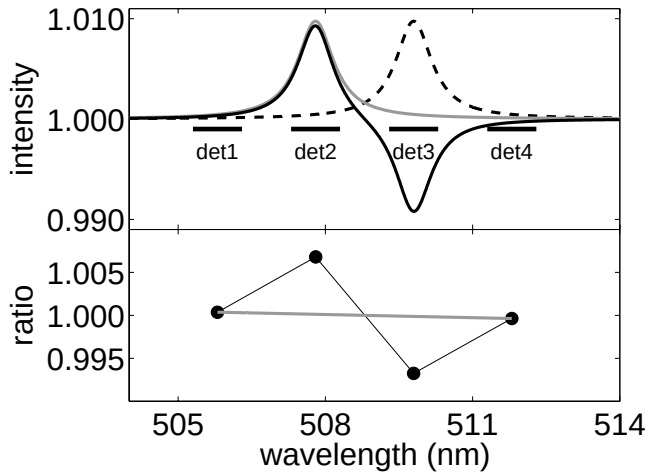


Figure 4. Top panel: the simulated Raman line with excitation at 473.0 nm (dashed line) and 471.3 nm (gray line) and the ratio of the two (black line). The short horizontal black lines represent the spectral pass bands of the analysis filters. Bottom panel: the values of the ratio of the two Raman signals in the top panel as measured by the four detectors, plotted versus filter wavelength (black circles) and the baseline (gray line). In skin measurements, the background has both slope and curvature (not shown in the figure).

Downloaded From: http://proceedings.spiedigitallibrary.org/ on 03/18/2014 Terms of Use: http://spiedl.org/terms

DSRS technique. We characterize the PMT response to 1% percent using a calibration LED with known brightness preceding each measurement. Absolute calibration is achieved by measuring the Raman response of a sample with known carotenoid concentration.

In a manufacturing setting, it is important to make sure the wavelengths are selected so that all machines are as spectrally similar as possible. In principle, non-equal wavelengths could be used in the detection channels (and in Eq. 1). If it was possible to derive a reliable lineshape model, then the specifications on the excitation wavelengths could also be relaxed. However, our studies indicate that different individuals show Raman shift variability by as much as 0.2 nm.

7. BENCHMARK COMPARISON TO LASER-BASED UNITS

Pharmanex® developed a Raman transfer standard which we use to set the intensity scale in our Raman measurements. We call the measured intensity an "antioxidant score." It is essentially an arbitrary scale, but in round numbers the average American has a score in the neighborhood of 25,000 for measurements made in the palm of the hand. Typical scores range from 10,000 to 50,000, similar to the spread of the population seen in Fig. 5 and the measurement uncertainty is less than 3,000.

We have performed hundreds of tests comparing the performance of our units and laser-based Raman spectrometers. The results of one test are shown in Fig. 5. For this study, 38 persons repeatedly measured their antioxidant scores on a laser Raman instrument and also on LED Raman instruments over a one week time period. To within the error of the measurements, the two different kinds of instruments read identically to one another. A straight-line fit to the data in Fig. 5 has a reduced R^2 value of 0.96. The LED Raman instruments also show high repeatability. The vertical errorbars in Fig. 5 are the 1σ standard deviations of 20 measurements on two LED Raman units. The average relative standard deviation (RSD) is 9%. This is the 1σ variation in a person's score divided by their mean score and averaged over the 38 persons in this study. The typical RSD is somewhat lower for scores in the 25000 to 50000 range.

The LED Raman instruments are accurate in spite of their low intensity illumination of the skin. The optical power on the skin is less than 0.5 mW in a 3.1 mm^2 area. The resulting maximum intensity is 0.016

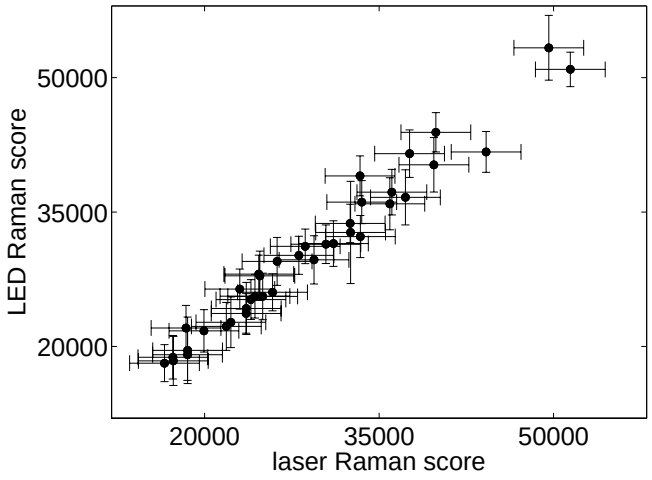


Figure 5. Comparison of laser-Raman and LED-Raman carotenoid measurements on 38 people. The vertical error bars are the 1σ standard deviations for 20 measurements on two LED Raman instruments over five days. The horizontal error bars are typical 1σ standard deviation measurements for the laser Raman instruments. The measurement time is two minutes for the LED Raman instrument and three minutes for the laser Raman instruments. To within the measurement uncertainty, this graph shows perfect correlation between the two machines. The reduced R^2 value of a straight line fit is 0.96.

Downloaded From: http://proceedings.spiedigitallibrary.org/ on 03/18/2014 Terms of Use: http://spiedl.org/terms

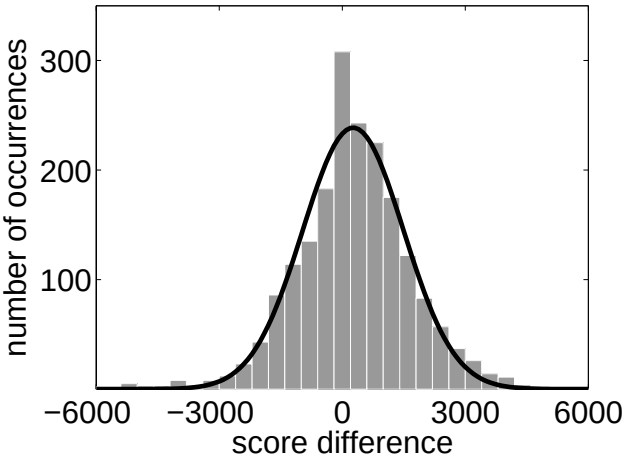


Figure 6. Histogram of score differences over a 265 day period. The x-axis is the difference between the scores determined using on-site calibration (147 different calibration events) and the scores determined using the internal calibration standards. The 1σ width (68.3% confidence level) determined by the Gaussian fit to the data (black line) is ± 1235.

W/cm^2, which is $12.5\times$ lower than the maximum permissible exposure for laser radiation of comparable wavelength.[16]

8. LONG-TERM CALIBRATION RELIABILITY

The LED Raman instruments are designed to have long-term calibration reliability. The optical system includes a photodiode to measure the brightness of the emission sources and also an additional LED and photodiode to measure the PMT sensitivity (not shown in Fig. 3). These items constitute a set of internal calibration standards for the instrument. They allow us to correct readings for drifts in excitation intensity and PMT sensitivity over time that may arise from temperature variation or component aging.

In normal use, a unit is calibrated at the beginning of a measurement session using a portable Raman standard. All of the PMT, LED, and photodiode values are recorded. Using the internal calibration standards, we correct all readings back to the LED brightness and PMT sensitivities as measured at the time of calibration.

The internal calibration standards are highly robust. Instead of using them to refer to conditions at the beginning of a particular measurement session, they can be used to refer to conditions at a factory calibration. In Fig. 6 we compare the scores measured over a 265 day period determined in two ways. The first is the "normal" way, using calibrations performed at the point of measurement. The second way uses the internal calibration standards to refer back to a single factory calibration. The data in Fig. 6 is a histogram of differences in the scores calculated in these two ways. The overall shift in score is approximately 1%. The 1σ confidence level (68.3%) is ± 1235. A closer evaluation of the data suggests that most of these score differences arise from errors in the calibration at the point of measurement. These data show that the internal calibration standards are stable over time periods approaching a year, and stability over much longer time periods seems likely.

9. CONCLUSION

We have developed a compact Raman spectrometer that uses LEDs excitation. Thousands of these have been built and are in routine operation. These units use two different bandwidth narrowed LED to excite the Raman spectrum and measure the sample fluorescence in four different analysis channels. We have

Downloaded From: http://proceedings.spiedigitallibrary.org/ on 03/18/2014 Terms of Use: http://spiedl.org/terms

shown repeatability better than 10% on LED Raman instruments and excellent correlation with laser-based Raman spectroscopy measurements. This work represents an important step forward for non-laboratory *in vivo* Raman spectroscopy using low intensity excitation. With the expanding availability of ultraviolet LEDs, and considering that many important biomolecules have resonances in the ultraviolet wavelength range, this approach may be useful for other systems.

REFERENCES

1. J. F. Dorgan, N. A. Boakye, T. R. Fears, R. L. Schleicher, W. Helsel, C. Anderson, J. Robinson, J. D. Guin, S. Lessin, L. D. Ratnasinghe, and J. A. Tangrea, "Serum carotenoids and α-tocopherol and risk of nonmelanoma skin cancer," *Cancer Epidemiol Biomarker and Prev.* **13**, 1276–1282 (2004).
2. W. Gellermann, I. V. Ermakov, M. R. Ermakova, and R. W. McClane, "*In vivo* resonant raman measurements of macular carotenoid pigments in the young and in the aging human retina," *J. Opt. Soc. Am. A* **19**, 19 (2002).
3. I. V. Ermakov, M. R. Ermakova, W. Gellermann, and J. Lademann, "Noninvasive selective detection of lycopene and β-carotene in human skin using raman spectroscopy," *J. Biomed. Opt.* **9**, 332–338 (2004).
4. P. J. Caspers, G. W. Lucasson, E. A. Carter, H. A. Bruining, and G. J. Puppels, "*I*n vivo confocal raman microspectroscopy of the skin: noninvasive determination of molecular concentration profiles," *J. Invest. Dermatol.* **116**, 434–442 (2001).
5. C. J. Frank, D. C. B. Redd, T. S. Gansler, and R. L. McCreery, "Characterization of human breast biopsy specimens with near-ir raman spectroscopy," *Anal. Chem.* **66**, 319–326 (1994).
6. T. R. Hata, T. A. Scholz, I. V. Ermakov, R. W. McClane, F. Khachik, W. Gellermann, and L. K. Pershing, "Non-invasive raman spectroscopic detection of carotenoids in human skin," *J Invest Dermatol* **115**, 441–448 (2000).
7. P. S. Bernstein, M. D. Yoshida, N. B. Katz, R. W. McClane, and W. Gellermann, "Raman detection of macular carotenoid pigments in intact human retina," *Invest Ophthalmol Vis Sci* **39**, 2003–2011 (1998).
8. T. Polivka and V. Sundstrom, "Ultrafast dynamics of carotenoid excited states – from solution to natural and artificial systems," *Chem. Rev.* **104**, 2021–2071 (2004).
9. J. Sue and S. Mukamel, "Analysis of fluorescence line shapes and raman excitation profiles of tetradesmethyl-β-carotene," *J. Chem. Phys.* **88**, 651–665 (1988).
10. R. R. Anderson and J. A. Parrish, "The optics of human skin," *J. Invest. Dermatol.* **77**, 13–19 (1981).
11. I. V. Ermakov, M. R. Ermakova, and W. Gellermann, "Simple Raman instrument for *in vivo* detectioni of macular pigments," Appl. Spectr. 59, 861–867 (2005).
12. S. E. J. Bell, E. S. O. Bourguignon, A. C. Dennis, J. A. Fields, J. J. McGarvey, and K. R. Seddon, "Identification of dyes on ancient Chinese paper samples using the subtracted shifted Raman spectroscopy method," *Anal. Chem.* **72**, 234–239 (2000).
13. S. D. Bergeson, J. B. Peatross, N. J. Eyring, J. F. Fralick, D. N. Stevenson, and S. B. Ferguson, submitted to J. Biomedical Opt.
14. I. V. Ermakov, R. W. McClane, and W. Gellermann, "Resonant raman detection of macular pigment levels in the living human retina," *Opt. Lett.* **26**, 202–204 (2001).
15. I. V. Ermakov, M. Sharifzadeh, M. Ermakova, and W. Gellermann, "Resonance Raman detection of carotenoid antioxidants in living human tissue," *J Biomed Opt* **10**, 064028 (2005).
16. American National Standards for the Safe Use of Lasers, ANSI Z136.1-2000, Table A3.

Downloaded From: http://proceedings.spiedigitallibrary.org/ on 03/18/2014 Terms of Use: http://spiedl.org/terms